Int. J. Nonlinear Anal. Appl. 9 (2018) No. 2, 21-31
ISSN: 2008-6822 (electronic)
http://dx.doi.org/10.22075/ijnaa.2018.12625.1641

Nonlinear dynamic of the multicellular chopper

Philippe Djondiné[a,b,*], Jean-Pierre Barbot[b]

[a]Department of Physics, Faculty of Science, The University of Ngaoundéré, P.O. Box 454, Ngaoundéré, Cameroon
[b]ECS-Lab, EA3649, ENSEA, Cergy Cedex, Cergy–Pontoise 95014, France, Laboratoire QUARTZ EA 7393

(Communicated by M. Eshaghi)

Abstract

In this paper, the dynamics of multicellular chopper are considered. The model is described by a continuous time three–dimensional autonomous system. Some basic dynamical properties such as Poincaré mapping, power spectrum and chaotic behaviors are studied. Analysis results show that this system has complex dynamics with some interesting characteristics.

Keywords: chaos; multicellular chopper, dynamical properties, chaotic attractor, routes to chaos.
2010 MSC: Primary 26A25; Secondary 39B62.

1. Introduction

A multilevel converter, which includes an array of power semiconductors and capacitor voltage sources, can synthesize a desired output voltage from several levels of dc voltages as inputs. With an increasing number of dc voltage sources, the converter output voltage waveform approaches a nearly sinusoidal waveform while using a fundamental frequency switching scheme [30]. The primary advantage of multilevel converters is generating high voltage with smaller steps at the output while the power semiconductors must withstand only reduced voltages; this will results in high power quality, lower harmonic components, better electromagnetic compatibility, and lower switching losses [29, 30, 33]. One of fundamental multilevel topologies is known as Multicell Converter, including Flying Capacitor Multicell (FCM) or serial multicellular, Stacked Multicell (SM), and Cascaded Multicell (CM) converters.
The serial multicellular converter has gained substantial interest in high power systems. It allows to synthesize high voltage multilevel waveforms using low voltage power semiconductors. The first serial multicellular converter was introduced in [28]. The power structure is an imbricated association of two or more commutation cells and flying capacitors, where the flying capacitor voltages determine

*Corresponding author
Email addresses: pdjondine@yahoo.fr (Philippe Djondiné), barbot@ensea.fr (Jean-Pierre Barbot)

Received: September 2017 *Revised:* January 2018

the output waveform quality and the safe converter operation. However, a high number of voltage levels increases the control complexity and introduces a capacitor voltage imbalance problem [30]. The capacitor imbalance problem can be addressed by open–loop or closed–loop control strategies. Open–loop schemes rely on the natural balancing property. Studies [22, 23, 32, 41, 43, 44] show that natural balancing will take place if the converter cells are commanded with symmetric pulse patterns. Moreover, natural voltage balancing dynamics improves if an auxiliary resonant resistive–capacitive-inductive circuit is connected in parallel with the load [25, 37, 38, 39], or by modifying the phase–shifted pulse width modulation scheme [17, 24, 26, 34, 40]. Approaches based on natural balancing are simple, but auxiliary circuits increase losses, and solutions relying on symmetric pulse patterns are risky due to errors introduced by non ideal electronic components and related implementation issues. Closed–loop or active control improves balancing properties using closed-loop control strategies.

In recent decades, it was discovered that most of static converters were the seat of unknown nonlinear phenomena in power electronics [7, 8, 13, 19]. It is for example the case of multicellular choppers that can exhibit unusual behaviors and sometimes chaotic behaviors. Obviously, this may generate dramatical consequences. However, the usually averaged models do not allow to predict nonlinear phenomena encountered. By nature, these models obscure the essential nonlinearities [42]. To analyses these strange behaviors, it is necessary to use a nonlinear hybrid dynamical model [1], [13]. There have been many methods for detecting chaos from order [4, 6]. Among them, routes to chaos [6], routes to chaos with phase portraits, first return map, Poincare sections, Lyapunov exponents [2], fast Lyapunov indicators [12], SAI (Smaller Alignment Index) [35] and its generalized alignment index [36], bifurcations, power spectra [3], frequency analysis [18], 0-1 test [15], geometrical criteria [16, 46], and fractal basin boundaries [20], and soon, are developed in the literature. Each of these methods has its advantages and drawbacks in classifying the attractors. The main purpose of the present paper is to propose a framework of chaotic behavior study for two–cells chopper connected to a nonlinear load. Three chaotic indicators, considered in the above literature, will be studied by using numerical approaches such as Matlab/Simulink in the case of multicell chopper. The paper is structured as follows. Section 2 deals with the modeling process. The electronic structure of the serial multicell chopper is addressed and the appropriate mathematical model is derived to describe the dynamics of the chopper. Two cells chopper modeling is then considered. Chaotic behavior and simulation results are presented in Section 3. Finally, some conclusion and remarks are reported in section 4.

2. Review of the multicellular converter and its operation

The multicellular converters (Figure 1) are built starting from an association of a certain number of cells. At the output, one obtains $(p+1)$ levels $(0, \frac{E}{p}, \ldots, \frac{(p-1)}{p}, E)$. This association in series allows to the output source V_s to evolve on $(p+1)$ possible levels. As the orders of the switches of the cells of commutation are independent, one obtains 2^p possible combinations. Thus, it is necessary to ensure an equilibrated distribution of the voltage of the floating condensers. Under these conditions, one obtains the following property:

The converter has $(p-1)$ floating voltages sources and the voltage of the capacity of index k is $k\frac{E}{p}$. The control signal associated with each commutation cell is noted as u_i where i_L represents the number of cells of the topology. This signal will be equal to 1 when the upper switch of the cell is conducting and 0 when the lower switch of the cell is conducting.

Note that the chopper, which has a purely dissipative load, cannot generate a chaotic behavior. Nevertheless, it is well known since from [27] that power converter when it is connected to nonlinear load may have a chaotic behavior. The chopper modeling is:

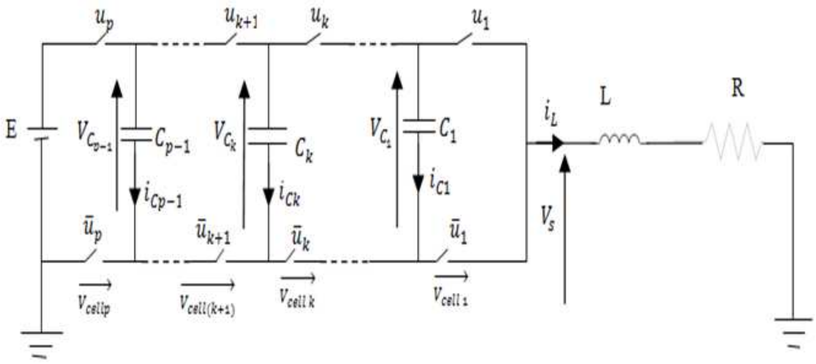

Figure 1: P-cells chopper connected to RL load

$$\begin{cases} \frac{dv_{C_1}}{dt} &= \frac{u_2-u_1}{C_1} i_L \\ \frac{dv_{C_2}}{dt} &= \frac{u_3-u_2}{C_2} i_L \\ \vdots & \\ \frac{dv_{C_{p-1}}}{dt} &= \frac{u_p-u_{p-1}}{C_{p-1}} i_L \\ \frac{di_L}{dt} &= \frac{u_1-u_2}{L} v_{C_1} + \frac{u_2-u_3}{L} v_{C_2} + \cdots \\ & \quad + \frac{u_{p-1}-u_p}{L} v_{C_{p-1}} + \frac{u_p}{L} E - \frac{R}{L} i_L. \end{cases} \tag{2.1}$$

To simplify the study and the notations, we will study the overlapping operation of a converter with two cells (Figure 2). Its function is to supply a passive load (RL) in series with another nonlinear load connected in parallel with a capacitor [9]. Four operating modes are then possible as shown in Figure 3. Note that the floating source takes part in the evolution of the dynamics of the system only to the third and fourth mode. In the third mode, the capacity discharges and charge during the fourth mode. Thus, if these two modes last same time with a constant charging current, then the average power transmitted by this floating source over one period of commutation is null. We also notice that these two modes make it possible to obtain by commutation the additional level $\frac{E}{2}$ on the output voltage V_s.

As the switches of each cell are regarded as ideals, their behavior can be to model by a discrete state taking of the values 0 (on) or 1 (off). In practice, some of these states never will be visited for reasons of safety measures or following the strategy of order adopted or because of the structure of the converter him finally to even or comply with the rule of adjacency. The transitions are not necessarily controlled.

The system model can be represented by three differential equations giving its state space:

$$\begin{cases} L\frac{di_L}{dt} &= (u_1-u_2)v_C - v_{C_l} - Ri_L + u_2 E \\ C\frac{dv_C}{dt} &= (u_2-u_1)i_L \\ C_l\frac{dv_{C_l}}{dt} &= i_L - g(v_{C_l}), \end{cases} \tag{2.2}$$

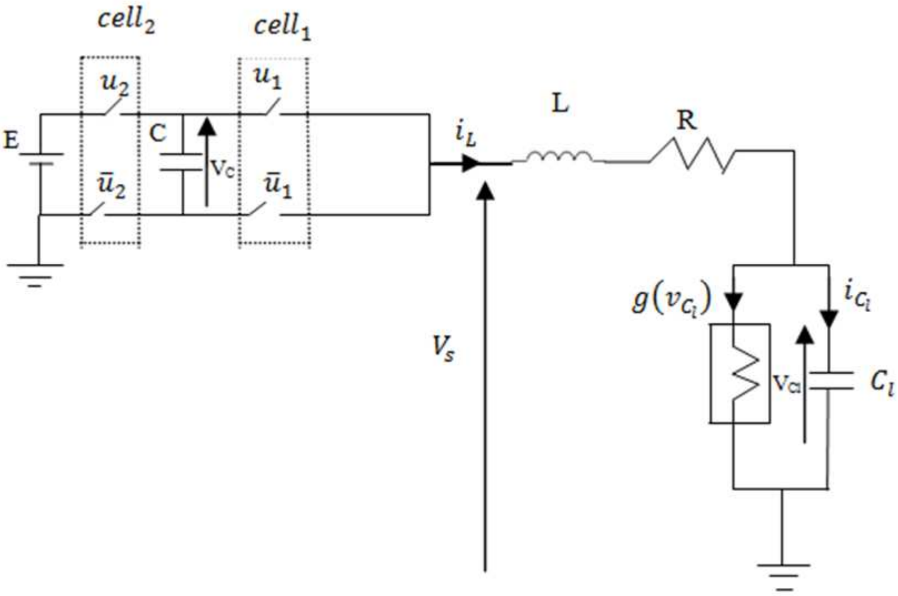

Figure 2: Two-cells chopper connected to a nonlinear load

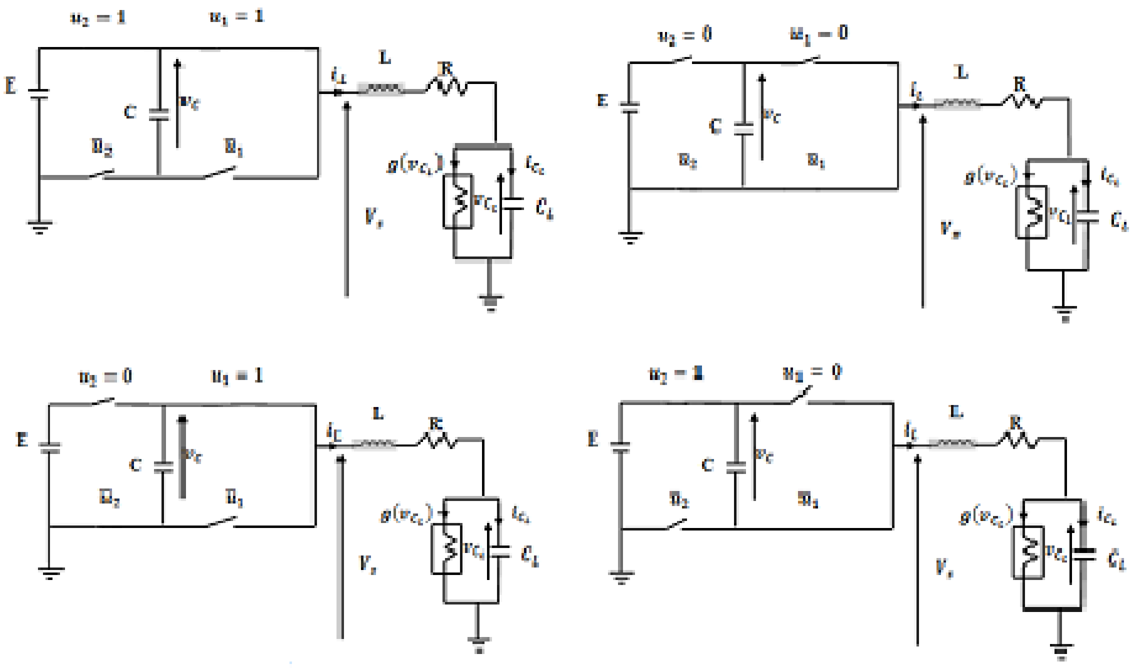

Figure 3: Two cell converter and its configurations

where

$$g(v_{C_l}) = G_b v_{C_l} + \frac{1}{2}(G_a - G_b)(|v_{C_l} + 1| - |v_{C_l} - 1|),$$

which is the mathematical representation of the characteristic curve of nonlinear load. The slopes of the inner and outer regions are G_a and G_b. The parameters of the circuit elements are fixed as $L = 50mH$, $C = 0.1\mu F$, $C_l = 40\mu F$, $E = 100V$.

3. Some basic properties of the multicellular chopper

For the power converters, many methods like phase portraits, bifurcation diagrams, and time–domain waveform can be used to analyze the nonlinear phenomenon in the system. In this work, the bifurcation diagrams and Poincaré sections are drawn based on the discrete iterated mapping model. Time–domain waveform, phase portraits, and power spectrum are obtained by building simulation module in Matlab/Simulink, which is analyzed from literature results. Rescaling equation (2.2) as $v_C = x_2 B_p, v_{C_l} = x_3 B_p, i_L = x_1 G B_p, G = \frac{1}{R}, t = \frac{C}{G}\tau$ and then redefining τ as t the following set of normalized equations are obtained:

$$\begin{cases} \dot{x}_1 &= \beta(\gamma x_1 + \epsilon x_2 + x_3) + \alpha E \\ \dot{x}_2 &= \epsilon x_1 \\ \dot{x}_3 &= p(x_1 - g(x_3)), \end{cases} \tag{3.1}$$

where $\epsilon = u_2 - u_1, p = \frac{C}{C_l}, \beta = \frac{C}{LG^2}, \gamma = RG, \alpha = \beta u_2$. Obviously $g(x_3) = bx_3 + 0.5(a-b)[|x_3+1| - |x_3-1|]$, or

$$g(x_3) = \begin{cases} bx_3 + a - b & x_3 > 1, \\ ax_3 & |x_3| \le 1, \\ bx_3 - a + b & x_3 < -1. \end{cases} \tag{3.2}$$

Now the dynamics of equation (3.1) depends on the parameters $\epsilon, p, \beta, \gamma, a, b$ and α. The circuit parameters used are then rescaled as: $p = 25.10^{-4}, a = -15, b = 5, \gamma = 1$ and β variable.

3.1. Dissipativity

Preliminary insights concerning the existence of attractive sets [45] that might coexist in the system could be gained by evaluating the volume contraction/expansion rate ($\wedge = V^{-1}\frac{dV}{dt}$ of the multicell chopper modeled by (3.1) at any given point $x = (x_1\, x_2\, x_3)^T$ of the state space. The following expression can be derived:

$$\wedge = \frac{\partial \dot{x}_1}{\partial x_1} + \frac{\partial \dot{x}_2}{\partial x_2} + \frac{\partial \dot{x}_3}{\partial x_3} = \begin{cases} -\beta\gamma - pb & |x_3| > 1, \\ -\beta\gamma - pa & |x_3| \le 1. \end{cases} \tag{3.3}$$

This means system (3.1) is dissipative system when $(\beta\gamma + pb) > 0$ or $(\beta\gamma + pa) > 0$. Note that $(-\beta\gamma - pb)$ is a negative value. Thus the volume elements are contracting. After a time unit this contraction reduces a volume V_0 by a factor $e^{-(\beta\gamma + pb)t}$. Which means that each volume containing the trajectory of this dynamical system converges to zero as $t \to \infty$ at exponential rate $(\beta\gamma + pb)$. Therefore, all system orbits are ultimately confined to a specific subset having zero volume and the asymptotic motion settles onto an attractor.

3.2. Symmetry and invariance

We can see the invariance of the system under the coordinate transformation $(x_1, x_2, x_3) \to (x_1, -x_2, x_3)$. Also note that, in the x_3 versus x_2 plane there is symmetry around the nominal value of the voltage of the floating capacitor that is 50V. This symmetry is shown in Figure 4. Parameters values are $p = 25.10^{-4}, \alpha = 2.10^{-2}(u_2 = 1), a = -15, b = 5, \gamma = 1$ and the initials values $(0, 5, 4)$.

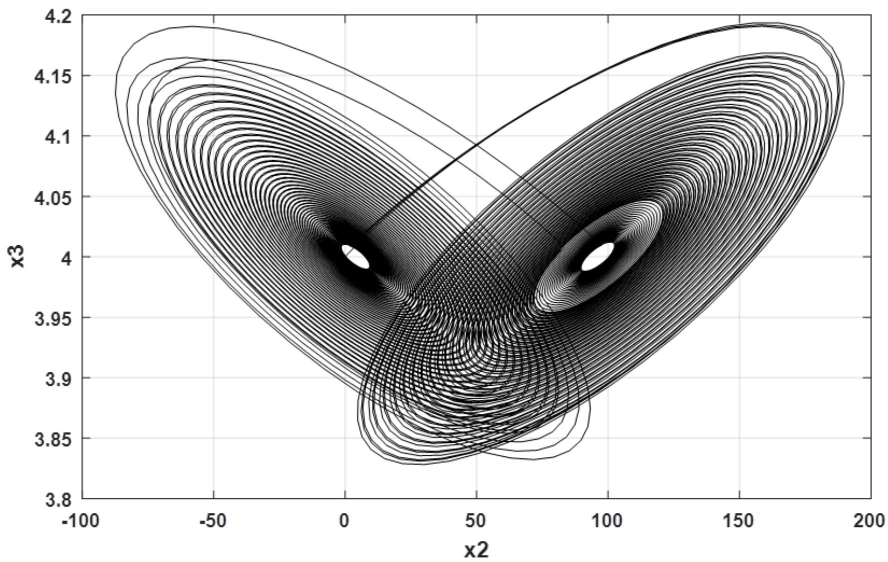

Figure 4: Phase plane strange attractors x_3 versus x_2

3.3. Chaotic behavior

System (3.1) is solved numerically to define routes to chaos in our model using the standard three–order Runge–Kutta algorithm. For set f_s (switching frequensy) parameters used in this work, the time step is always $\triangle t = 0.005$ and computation are performed using variables and constants parameters extended mode. For each parameter combination, the system is integrated for a sufficiently long time and transient is discarded. Three indicators are used to identify the type of transition leading to chaos. The first indicator is the Poincaré section, the second is a first return map and the third is the routes to chaos.

We now focus on the effects biasing on the dynamics of the two cells chopper connected to a nonlinear load modeled by equation (2.2). To achieved this goal, R or β is chosen as control parameter and the rest of system parameters are assigned the values: $p = 25.10^{-4}, \alpha = 2.10^{-2}, a = -15, b = 5, \gamma = 1$.

3.3.1. Poincaré section

To distinguish between chaos and quasi–periodicity, we need a special tool to uncover the hidden information contained in the steady–state trajectory of a system (i.e. attractor). The tool we use is called Poincaré section, which is a two dimensional plane that intersects the trajectory. By examining the way in which the steady–state trajectory intersects an appropriately chosen Poincaré section, we can tell if the steady–state operation is periodic, quasi–periodic or chaotic.

The Poincaré section is computed for $x_1 = 0$ when $R = 10\Omega$ [10, 11]. From Figure 5 it can be seen that the symmetry is around the nominal voltage capacitor V_{C_n} [14]. We also see a local symmetry around the floating capacitor voltages 0 and 100.

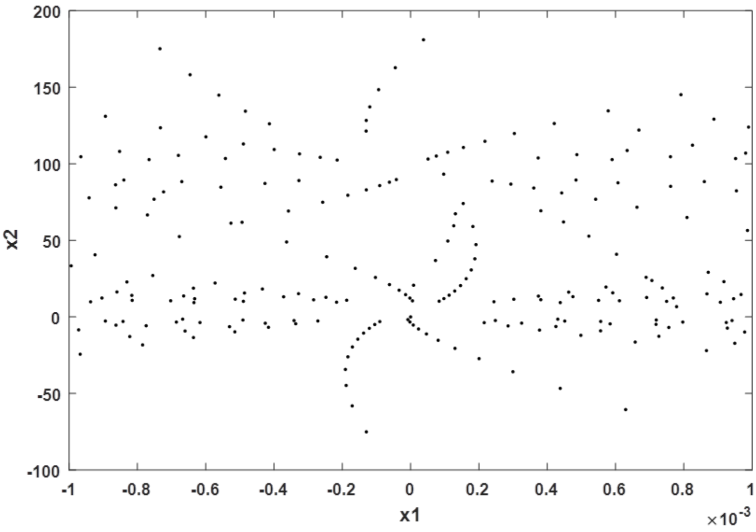

Figure 5: The Poincaré section of x_1 versus x_2 plane

3.3.2. First return map

Another tool which illustrates the interesting dynamics of two cells chopper attractor is the Poincaré first return map. We again take a cross section of the band by cutting through it with a plane perpendicular to the flow (for our purposes the portion of the x_1 versus x_3 plane with $|x_1| < 0.01$ works well). We then record the x_3 value of a trajectory when it crosses our plane and graph it against the x_3 value of the next time the trajectory crosses the section. In this way we can investigate the mixing which is done by the twist in the attractor. From Figure 6 it can be seen that there is a folding point at each end of the cross and obviously symmetry occurs.

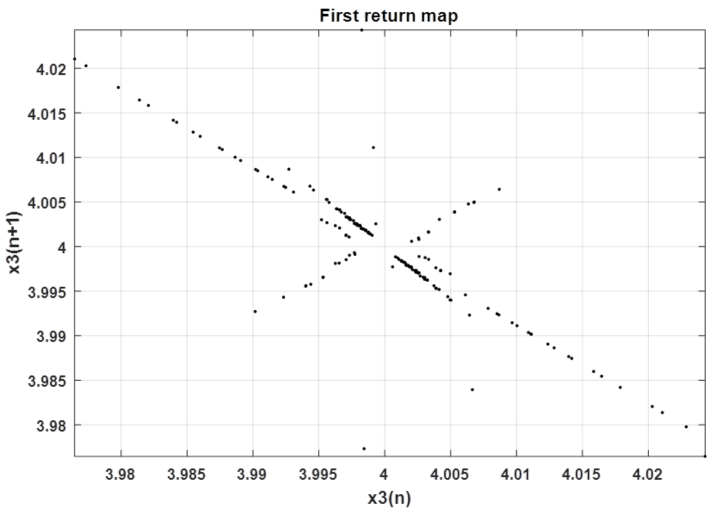

Figure 6: First return map

3.3.3. Routes to chaos

This nonlinear system exhibits the complex and abundant chaotic dynamics behaviors, the strange attractors are shown in Figures 7 and 8. These phase portrait are obtained by solving equations (2)

to (3) by means of Runge Kutta method for step size of 0.000001.
One of the routes to chaos observed in studied multicellular chopper is scroll doubling, which continues until there are no further stable states. At the beginning of simulation $u_1 = u_2 = 0$.
Now it is clear that the double scroll attractor has a structure quite different from the well–known Lorenz [21], Rössler [31] and the Chua [5] attractors since the double–scroll structure has not been observed with the latter attractors.
During system parameter changes, periodic state becomes unstable because of period doubling scroll. Between 1Ω and 50Ω, one has a double scroll centered around the equilibrium points. From 100Ω (Figure 7 (e)), the second scroll tends to disappear.
For $R = 1000\Omega$ and $R = 1500\Omega$, the attractor evolves in to the limit cycles; the limit cycles are shown in Figure 8 (g) and Figure 8 (h).
The spectrum of this nonlinear system (2) is studied; its spectrum is continuous as show in Figures 7 and 8. We observe from these figures that the system exhibits chaotic behaviors.

4. Conclusions

In this paper, the dynamics properties of multicellular chopper have been investigated using numerical methods. The first return map, Poincaré sections and routes to chaos were used as indicators of chaotic behaviors. These indicators show that this system can have chaotic behaviors. These new attractors are different from the Lorenz attractor, Rossler and Chua, but it is a butterfly shaped chaotic attractor.

References

[1] J.P. Barbot, H. Saadaoui and N. Manamanni, *Nonlinear observer for autonomous switching systems with jump*, Nonlinear Anal. Hybrid Syst. 1 (2007) 537–547.
[2] G. Benettin, L. Galgani and J. M. Strelcyn, *Kolmogorov entropy and numerical experiments*, Phys. Rev. A 14 (1976) 2338–2445.
[3] J. Binney and D. Spergel, *Spectral stellar dynamics*, Astrophys. J. 252 (1982) 308–321.
[4] G. Chen and X. Dong, *From chaos to order: Methodologies, perspectives and applications*, World Scientific Series on Nonlinear Science Series A, 24(ISBN: 978-981-02-2569-8), 776 pages, 1998.
[5] L.O. Chua, *Chua's Circuit: An Overview Ten Years Later*, J. Circuit. Syst. Comp. 4 (1994) 117–159.
[6] G. Contopoulos, *Order and chaos in dynamical astronomy*, Springer Verlag, 2002.
[7] F. Defay, A.M. Llor and M. Fadel, *A predictive control with flying capacitor balancing of a multicell active power filter*, IEEE Trans. Ind. Electron. 55 (2008) 3212–3220.
[8] M. Di Bernardo and K. T. Chi, *Bifurcation and chaos in power electronics: an overview in nonlinear dynamics in engineering*, Edited by Prof. G. Chen and T. Ueta, World Scientific, 317–340, 2002.
[9] P. Djondiné, R. He, M. Ghanes and J.-P. Barbot, *Chaotic behavior study for serial multicellular chopper connected to nonlinear load*, Proceedings of the 3rd International Conference on Systems and Control, Algiers, Algeria, October 29–31, 2013.
[10] P. Djondiné, J.-P. Barbot and M. Ghanes, *Nonlinear phenomena study in serial multicell chopper*, In 4th IFAC Conference on Analysis and Control of Chaotic Systems, 2015.
[11] P. Djondiné, M. Ghanes, J.P. Barbot and B. Essimbi, *Dynamical behaviors of multicellular chopper*, J. Control Sci. Eng. 2 (2014) 35–42.
[12] C. Froeschlé , E. Lega and R. Gonczi, *Fast lyapunov indicators. applications to asteroidal motion*, Celest. Mech. Dyn. Astron. 67 (1997) 41–62.
[13] M. Ghanes, M. Trabelsi, X.L. Shi, J.P. Barbot, J.M. Retif and K. Busawon *High gain observer for a three–cell chopper: Design and experimental results*, Internat. J. Robust Nonlinear Control 24 (2013) 1090–1103.
[14] R. Gilmore and C. Letellier, *The symmetry of chaos*, Oxford University Press, USA, 2007.
[15] G.A. Gottwald and I. Melbourne, *A new test for chaos in deterministic systems.* Proc. R. Soc. London Ser. A 460 (2004) 603–611.
[16] L. Horwitz, Y.B. Zion, M. Lewkowicz, M. Schiffer and J. levitan, *Geometry of hamiltonian chaos*, Phys. Rev. Lett. 98 (2007) 234–301.

[17] D.W. Kang, B.K. Lee, J.H. Jeon, T.J. Kim and D.S. Hyun, *A symmetric carrier technique of CRPWM for voltage balance method of flying–capacitor multilevel inverter*, IEEE Trans. Ind. Electron. 52 (2005) 879–888.

[18] J. Laskar, *The chaotic motion of the solar system: A numerical estimate of the size of the chaotic zones*, Icarus 88 (1990) 266–291.

[19] J.I. Leon, R. Portillo, S. Vazquez, J.J. Padilla, L.G. Franquelo and J. M. Carrasco *Simple unified approach to develop a time–domain modulation strategy for single–phase multilevel choppers*, IEEE Trans. Ind. Electron. 55 (2008) 3239–3248.

[20] J. Levin, *Gravity waves, chaos, and spinning compact binaries*, Phys. Rev. Lett. 84 (2000) 3515.

[21] E.N. Lorenz, *Deterministic no periodic flow*, J. Atmos. Sci. 20 (1963) 130–141.

[22] B.P. McGrath and D.G. Holmes, *Analytical determination of the capacitor voltage balancing dynamics for three–phase flying capacitor converters*, IEEE Trans. Ind. Appl. 45 (2009) 1425–1433.

[23] B.P. McGrath and D.G. Holmes, *Analytical modelling of voltage balance dynamics for a flying–capacitor multilevel converter*, IEEE Trans. Power Electron. 23 (2008) 543–550.

[24] B.P. McGrath and D.G. Holmes, *Enhanced voltage balancing of flying capacitor multilevel converter using phase disposition (PD) modulation*, IEEE Trans. Power Electron. 26 (2011) 1933-1942.

[25] B.P. McGrath and D.G. Holmes, *Natural capacitor voltage balancing for a flying capacitor converter induction motor drive*, IEEE Trans. Power Electron. 24 (2009) 1554–1561.

[26] B.P. McGrath, T. Meynard, G. Gateau and D.G. Holmes, *Optimal modulation of flying capacitor and stacked multicell converters using a state machine decoder*, IEEE Trans. Power Electron. 22 (2007) 508–516.

[27] T.A. Meynard, M. Fadel and N. Aouda, *Modeling of multilevel converters*, IEEE Trans. Ind. Electronics 44 (1997) 356–364.

[28] T.A. Meynard and H. Foch, *Multilevel choppers for high voltage applications*, EPE Journal 2 (1992) 45–50.

[29] A. Nabae, I. Takahashi and H. Akagi, *A New Neutral-Point-Clamped PWM Inverter*, IEEE Trans. Ind. Appl. 17 (1981) 518–523.

[30] J. Rodriguez, J.S. Lai and F.Z. Peng, *Multilevel inverters: A survey of topologies, controls, and applications*, IEEE Trans. Ind. Electron. 49 (2002) 724–738.

[31] O.E. Rossler, *An equation for continuous chaos*, Phys. Lett. A 57 (1976) 397–398.

[32] A. Ruderman, B. Reznikov and M. Margaliot, *Simple analysis of a flying–capacitor converter voltage balance dynamics for dc modulation*, in Proc. IEEE Power Electron. Motion Control Conf. Sep. 2008, pp. 260–267.

[33] M. Sadeghi, S.H. Hosseini, R. Alizadeh and M.R. Banaei, *New Mixed Stacked Multicell Converter with Interesting Advantages*, IET power electronic (PEL) 5 (2012) 1298–1304.

[34] A. Shukla, A. Ghosh and A. Joshi, *Natural balancing of flying capacitor voltages in multicell inverter under PD carrier–based PWM*, IEEE Trans. Power Electron. 26 (2011) 1682–1693.

[35] C. Skokos, *Alignment indices: A new, simple method for determining the ordered or chaotic nature of orbits* J. Phys. A 34 (2001) 10029–10043.

[36] C. Skokos, T. Bountis and C. Antonopoulos, *Geometrical properties of local dynamics in hamiltonian systems: The generalized alignment index (gali) method*, Physica D 231 (2007) 30–54.

[37] R. Stala, *The switch–mode flying–capacitor DC–DC converters with improved natural balancing*, IEEE Trans. Ind. Electron. 57 (2010) 1369–1382.

[38] R. Stala, S. Pirog, M. Baszynski, A. Mondzik, A. Penczek, J. Czekonski and S. Gasiorek, *Results of investigation of multicell converters with balancing circuit–Part I*, IEEE Trans. Ind. Electron. 56 (2009) 2610–2619.

[39] R. Stala, S. Pirog, A. Mondzik, M. Baszynski, A. Penczek, J. Czekonski and S. Gasiorek, *Results of investigation of multicell converters with balancing circuit–Part II*, IEEE Trans. Ind. Electron. 56 (2009) 2620–2628.

[40] S. Thielemans, A. Ruderman, B. Reznikov and J. Melkebeek, *Improved natural balancing with modified phase–shifted PWM for single–leg five level flying–capacitor converters*, IEEE Trans. Power. Electron. 27 (2012) 1658–1667.

[41] S. Thielemans, A. Ruderman, B. Reznikov and J. Melkebeek, *Simple time–domain analysis of a four–level H–bridge converter voltage balancing*, in Proc. IEEE Int. Technol. Mar. 2010, pp. 818–823.

[42] C.K. Tse, *Complex behavior of switching power converter*, CRC Press, 2003.

[43] R.H. Wilkinson, T.A. Meynard and H. du Toit Mouton, *Natural balance of multicell converters: The two cell case*, IEEE Trans. Power Electron. 21 (2006) 1649–1657.

[44] R.H. Wilkinson, T.A. Meynard and H. du Toit Mouton, *Natural balance of multicell converters: The general case*, IEEE Trans. Power Electron. 21 (2006) 1658–1666.

[45] S. Wiggins, *Introduction to applied nonlinear dynamical systems and chaos*, Vol. 2. Springer Science, Business Media, 2003.

[46] X. Wu, *Is the hamiltonian geometrical criterion for chaos always reliable*, J. Geom. Phys. 59 (2009) 1357–1362.

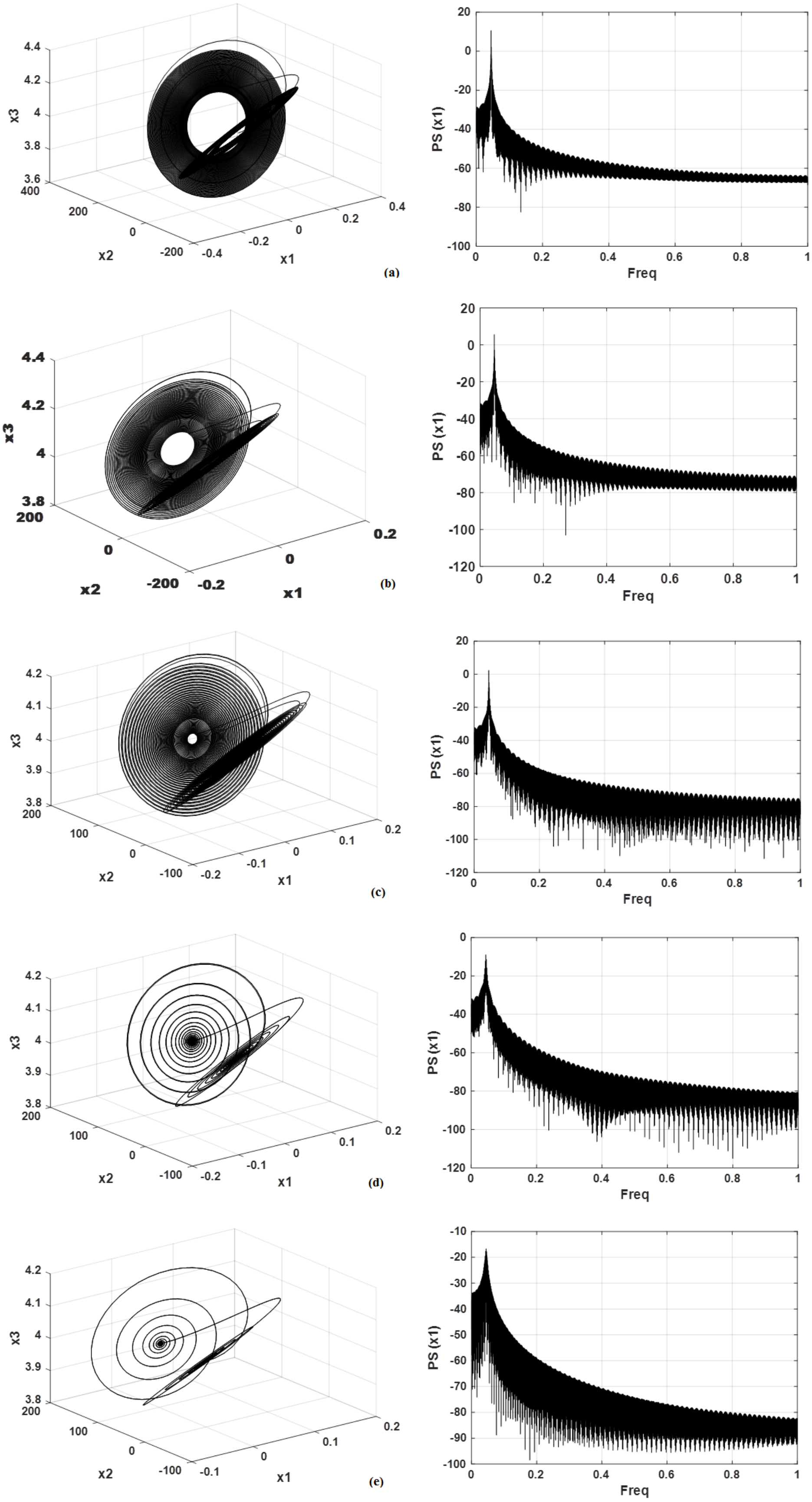

Figure 7: phase portraits: $(a) : R = 1\Omega, (b) : R = 5\Omega, (c) : R = 10\Omega, (d) : R = 50\Omega, (e) : R = 100\Omega$

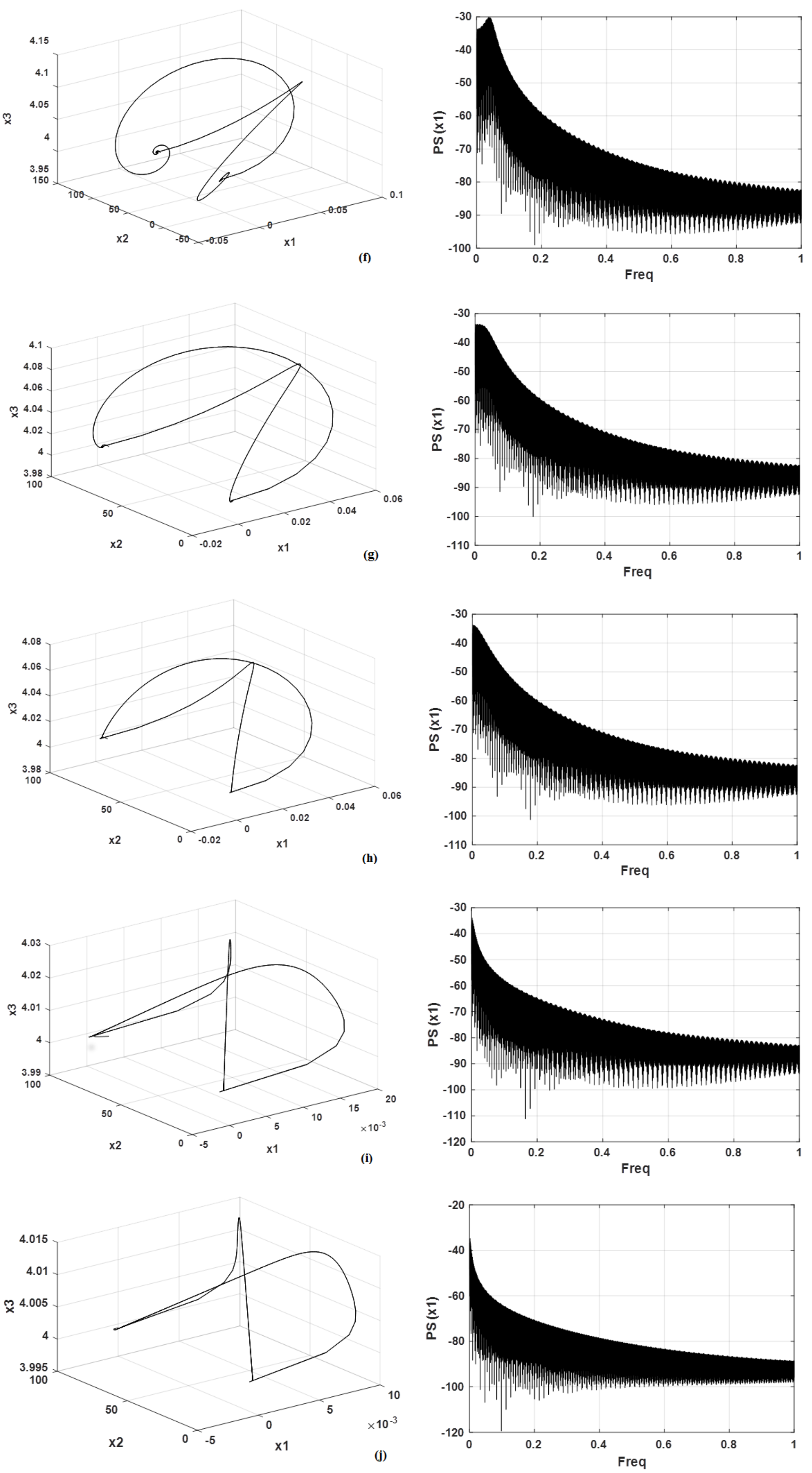

Figure 8: phase portraits: (suite) $(f) : R = 500\Omega, (g) : R = 1000\Omega, (h) : R = 1500\Omega, (i) : R = 5000\Omega, (j) : R = 10000\Omega$